Second mode transition in microstructured optical fibers: determination of the critical geometrical parameter and study of the matrix refractive index and effects of cladding size

Gilles Renversez and Frédéric Bordas

Université Paul Cézanne Aix-Marseille III and Institut Fresnel (Unité Mixte de Recherche 6133, Centre National de la Recherche Scientifique), Faculté des Sciences et Techniques de St Jérôme, Avenue Escadrille Normandie-Niémen, 13397 Marseille Cedex 20, France

Boris T. Kuhlmey

Centre for Ultrahigh-Bandwidth Devices for Optical Systems and School of Physics, University of Sydney, Sydney, NSW 2006, Australia

Received November 17, 2004

We carried out a numerical study of the second mode transition in finite-sized, microstructured optical fibers (MOFs) for several values of the matrix refractive index. We determined a unique critical geometrical parameter for the second mode cutoff that is valid for all the matrix refractive indices studied. Finite size effects and extrapolated results for infinite structures are described. Using scaling laws, we provide a generalized phase diagram for solid-core MOFs that is valid for all refractive indices, including those of the promising chalcogenide MOFs. © 2005 Optical Society of America

OCIS codes: 060.2270, 060.2280, 060.2400, 060.2430.

Arguably, the most striking property of microstructured optical fibers (MOFs) is that they can be endlessly single mode.[1] In conventional step-index fibers there exist a finite number of modes that are strictly guided, characterized by the fact that their propagation constants β are real. All other modes are leaky, with propagation constants that have nonzero imaginary parts. The number of guided modes increases with decreasing wavelength, and it is only at wavelengths longer than the cutoff wavelength that the fiber is single mode.[2,3] In contrast, ideal (or infinite) solid-core MOFs, which consist of single defects in infinite two-dimensional photonic crystals, can remain single mode at all wavelengths if the holes are sufficiently small.[4,5] Those fibers are said to be endlessly single mode.

Previous studies of the second mode cutoff in MOFs have led to a so-called phase diagram that partitions the parameter space into three regions, depending on whether the MOF is single mode, multimode, or endlessly single mode. However, this phase diagram was established solely for silica MOFs.[4,6] Given that MOFs can be made from a variety of dielectrics and that some of the most promising MOF applications, notably nonlinear ones, rely on high-refractive-index materials such as chalcogenides,[7] it is important to know whether high-index solid-core MOFs can exhibit the endlessly single-mode property within a realistic range of fiber parameters and wavelengths. We numerically investigate the effect of matrix refractive index n_{mat} of the MOF's matrix material on the phase diagram by using the multipole method.[6,8] We accurately determine the critical relative hole size that delimits the endlessly single-mode region, which is independent of n_{mat}.

Our studies also highlight finite size effects, which were ignored in previous studies and have an effect on the precise value of the critical relative hole size that delimits the endlessly single-mode region. Finally, using approximate scaling laws for binary step-index structures, we derive a generalized phase diagram that is valid for a large range of refractive-index contrasts.

We consider solid-core MOFs consisting of a finite number N_r of rings of triangularly arranged holes with circular cross sections (diameter d, refractive index n_i) in an infinite matrix (refractive index, n_{mat}); the core is a missing hole at the center. The center-to-center distance between holes (the pitch) is denoted Λ and is fixed at a value of 2.3 μm, and the effective index of modes is defined as $n_{\mathrm{eff}}=\beta/k_0$, in which $k_0=2\pi/\lambda$ is the free-space wave number and λ denotes the wavelength. We study the second mode cutoff of such MOFs to define their phase diagram in parameter space $(d/\Lambda, \lambda/\Lambda)$.

For such MOFs with finite N_r, the cutoff is not so clearly defined as for infinite MOFs. Indeed, in that case all modes are leaky; their propagation constants have nonzero imaginary parts. For these fibers the cutoff is a transition between two states of the same mode, one localized in the core and the other extending into the cladding. This transition has been studied, e.g., in terms of the sudden expansion of the second mode's effective area[5] or, equivalently, in terms of

0146-9592/05/111264-3/$15.00

a qualitative change of behavior of losses as a function of wavelength.[4] Here we use the latter definition of the cutoff, relying on peaks of quantity Q, defined here as

$$Q = \frac{\partial^2[\log \Im\mathrm{m}(n_{\mathrm{eff}})]}{\partial[\log \lambda]^2}, \tag{1}$$

in which $\Im\mathrm{m}(n_{\mathrm{eff}})$ is the imaginary part of n_{eff}. Quantity Q is related to the curvature in a log–log plot of the losses as a function of wavelength, and its peaks are associated with qualitative changes in the nature of the mode. For a detailed discussion of the meaning of Q we refer the reader to Refs. 4, 6, 9, and 10. n_{eff} is the effective index of the second mode and was computed by the multipole method.[6,8,11]

First, we concentrate on MOFs with a high matrix refractive index, $n_{\mathrm{mat}}=2.5$. Figure 1 shows Q as a function of normalized wavelength λ/Λ for various diameter-to-pitch ratios; $N_r=7$. The minimum of those curves precisely defines the normalized cutoff wavelength $(\lambda/\Lambda)_{\mathrm{S.M.}}$.[4] Further, as the Q peaks reflect the change of slope of $\Im\mathrm{m}(n_{\mathrm{eff}})$, the larger and narrower the peaks are, the sharper the transition between confined and unconfined modes is. Whereas in the research reported in Ref. 4 the Q minima were studied at fixed N_r, it appears that the behavior of the Q curves depends on N_r, as shown in Figs. 2 and 3. Figure 2 shows Q as a function of the normalized wavelength for two values of d/Λ, N_r ranging from 7 to 12, and $n_{\mathrm{mat}}=2.5$. For the same matrix index the magnitude of the Q minima $|Q_{\mathrm{min}}|$ as a function of N_r is shown in Fig. 3 for four d/Λ ratios.

Depending on the value of d/Λ, two different behaviors can be distinguished: for d/Λ ratios greater than or equal to 0.425 the minimum of Q becomes narrower (complete study not shown) and deeper with increasing N_r. Figure 3 shows that, in that case, $|Q_{\mathrm{min}}|$ diverges with N_r and, as can be seen from the curve for $d/\Lambda=0.43$, the rate at which $|Q_{\mathrm{min}}|$ diverges increases quickly with d/Λ. The divergence of $|Q_{\mathrm{min}}|$ implies that the cutoff transition becomes sharper

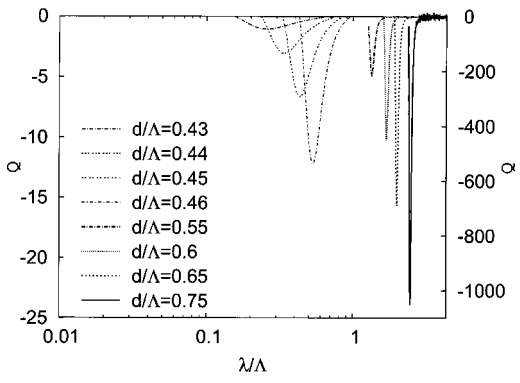

Fig. 1. Q as a function of normalized wavelength λ/Λ for eight d/Λ ratios for a seven-ring MOF made from a high–index matrix ($n_{\mathrm{mat}}=2.5$) with $\Lambda=2.3$ μm. Thinner curves (left) are associated with the left-hand y scale (lowest d/Λ and $|Q|$ values); the thicker curves use the right-hand y scale.

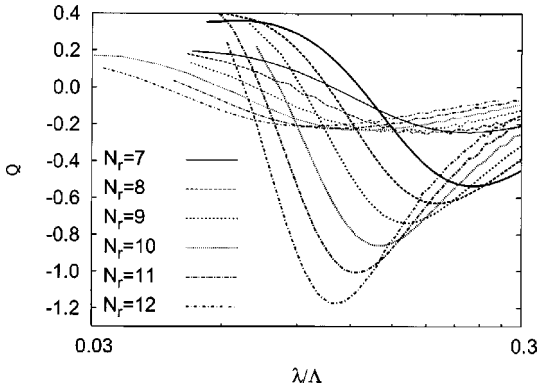

Fig. 2. Q as a function of λ/Λ for $d/\Lambda=0.42$ (thinner curves) and for $d/\Lambda=0.425$ (thicker curves) for several values of N_r.

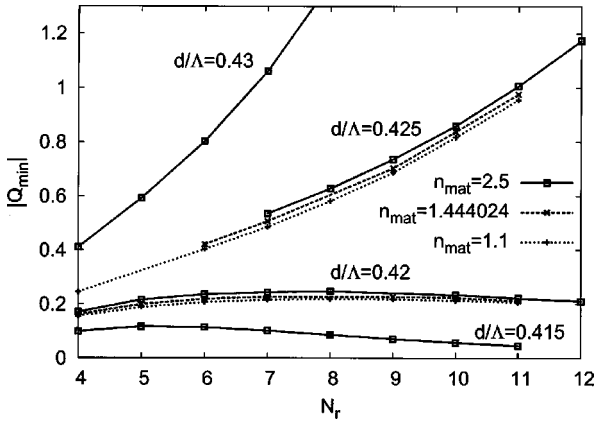

Fig. 3. $|Q_{\mathrm{min}}|$ as a function of N_r for three values of matrix index n_{mat} for several close d/Λ values.

with increasing numbers of rings, consistent with the fact that the cutoff should be infinitely sharp for infinite N_r.[9] Consequently the second mode does undergo a cutoff at finite wavelength for infinite MOFs with $d/\Lambda \geqslant 0.425$.

For $d/\Lambda=0.420$ and d/Λ ratios below this value, however; the minimum of Q vanishes slowly with increasing N_r. This behavior indicates that no transition should occur for the infinite MOF and therefore that the infinite MOF is endlessly single mode for $d/\Lambda \leqslant 0.420$. The critical value $(d/\Lambda)_{\mathrm{S.M.}}$ below which the MOF is endlessly single mode must therefore lie in the interval [0.420, 0.425].

Second, we investigate the effect of n_{mat} on the second mode transition. We repeat the above analysis of Q behavior for $n_{\mathrm{mat}}=1.1$ and $n_{\mathrm{mat}}=1.444024$ (Fig. 3). In all cases $(d/\Lambda)_{\mathrm{S.M.}}$ is strictly bounded by 0.420 and 0.425. Hence, from a numerical point of view, $(d/\Lambda)_{\mathrm{S.M.}}$ can depend only weakly on the matrix index; the theoretical aspects of this critical value are briefly discussed at the end of this Letter. $(d/\Lambda)_{\mathrm{S.M.}}$ can be considered a critical geometrical parameter associated with the second mode cutoff or similarly with the endlessly single-mode behavior of MOFs. Note that $n_{\mathrm{mat}}=1.444024$ was used in Ref. 4, in which $(d/\Lambda)_{\mathrm{S.M.}}$ was found to be 0.406. However, in that Letter a different criterion to establish the endlessly

single-mode limit was used, based on a study at fixed N_r. The fact that the Q minima disappear with increasing N_r at values close to but greater than 0.406 had been overlooked.

Third, we sum all our numerical results in the MOF parameter space $(d/\Lambda, \lambda/\Lambda)$. Figure 4 shows a phase diagram of the second mode [i.e., $(\lambda/\Lambda)_{\mathrm{S.M.}}$ as a function of d/Λ] for the three matrix indices studied, obtained for $N_r=7$, along with the extrapolated phase diagram for the infinite MOF with $n_{\mathrm{mat}}=2.5$ that results from an extrapolation of the $(\lambda/\Lambda)_{\mathrm{S.M.}}$ data computed for several values of N_r by use of a nonlinear least-squares algorithm. Note that for values of d/Λ close to $(d/\Lambda)_{\mathrm{S.M.}}$ the cutoff curves for finite and infinite N_r differ substantially. One must keep in mind that $(\lambda/\Lambda)_{\mathrm{S.M.}}$ is defined by the Q minimum and not directly by $\Im\mathrm{m}(n_{\mathrm{eff}})$. The nontrivial behavior of $(\lambda/\Lambda)_{\mathrm{S.M.}}$ with N_r should be studied by use of a W-profile fiber model, for example.

Increasing the index contrast shifts the cutoff curve toward longer wavelengths; however, the limit of the endlessly single-mode regime is conserved. Birks's analysis of scaling laws of photonic states with refractive-index contrast[12] shows that if λ, Λ, n_{mat}, or n_i varies, photonic states change, such that quantity $\nu=2\pi\Lambda(n_{\mathrm{mat}}^2-n_i^2)^{1/2}/\lambda$ remains invariant within the scalar approximation: For two structures with fixed d/Λ but different n_{mat} and n_i (say, n_{mat} and n_i and n'_{mat} and n'_i, respectively), the cutoff will occur at different wavelengths λ and λ' to keep ν constant at a value of $\nu_{\mathrm{S.M.}}$. Following this argument, we have

$$(\lambda/\Lambda)_{\mathrm{S.M.}}' = (\lambda/\Lambda)_{\mathrm{S.M.}}\left(\frac{n_{\mathrm{mat}}'^2 - n_i'^2}{n_{\mathrm{mat}}^2 - n_i^2}\right)^{1/2}. \qquad (2)$$

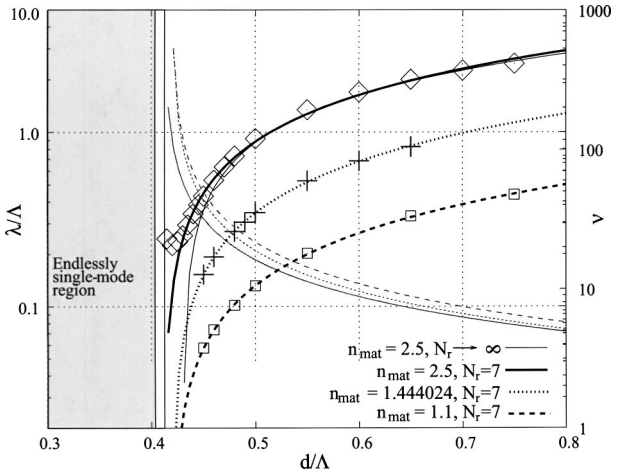

Fig. 4. Phase diagram for the second mode. The points correspond to the computed values of $(\lambda/\Lambda)_{\mathrm{S.M.}}$ for the three matrix indices for $N_r=7$; the thicker curves, to the fits. The thinner, solid curve is associated with the fit of the extrapolated results for $N_r\to\infty$ computed for $n_{\mathrm{mat}}=2.5$. The shaded region is the approximate endlessly single-mode region valid for the three matrix indices for $N_r\geq 7$. Lighter curves (right-hand scale) show the value of ν at cutoff for the same refractive indices as the corresponding darker curves.

We can hence draw a unified phase diagram by using quantity ν instead of λ/Λ (Fig. 4, lighter curves): MOFs with ν values that lie above the $\nu_{\mathrm{S.M.}}$ curve are multimode, whereas MOFs with ν values below the $\nu_{\mathrm{S.M.}}$ curve are single mode. As can be seen from Fig. 4, the $\nu_{\mathrm{S.M.}}$ curves for different n_{mat} are surprisingly consistent. (Keep in mind that the scaling laws used are valid only within the scalar approximation.) Furthermore, in the limit $\lambda\to 0$, the scalar approximation applied to the MOF becomes exact, and Eq. (2) is exactly verified. Consequently, the critical geometrical ratio $(\lambda/\Lambda)_{\mathrm{S.M.}}$ associated with the limit case $\lambda\to 0$ is necessarily the same for all the indices studied (see Refs. 1, 2, and 12 for the details of the scalar approximation).

In conclusion, we have explicitly shown that the ratio $(d/\Lambda)_{\mathrm{S.M.}}$ that delimits the endlessly single-mode regime in solid-core MOFs is independent of the matrix refractive index and can therefore be considered a critical geometrical parameter for the second mode cutoff. We observed that the differences between the behavior of finite and infinite structures are more pronounced near $(d/\Lambda)_{\mathrm{S.M.}}$. We have derived a generalized phase diagram for solid-core MOFs. In particular, our results demonstrate that the endlessly single-mode region is preserved for the promising chalcogenide MOFs.

This research benefited from travel support from the French and Australian governments and was produced with the assistance of the Australian Research Council. We thank the Free Software Foundation and Scilab consortium for their help. G. Renversez's e-mail address is gilles.renversez@fresnel.fr.

References

1. T. A. Birks, J. C. Knight, and P. St. J. Russell, Opt. Lett. **22**, 961 (1997).
2. A. W. Snyder and J. D. Love, *Optical Waveguide Theory* (Chapman & Hall, New York, 1983).
3. D. Marcuse, *Theory of Dielectric Optical Waveguides*, 2nd ed. (Academic, San Diego, Calif. 1991).
4. B. T. Kuhlmey, R. C. McPhedran, and C. M. de Sterke, Opt. Lett. **27**, 1684 (2002).
5. N. A. Mortensen, Opt. Express **10**, 341 (2002).
6. F. Zolla, G. Renversez, A. Nicolet, B. Kuhlmey, S. Guenneau, and D. Felbacq, *Foundations of Photonic Crystal Fibres* (Imperial College Press, London, 2005).
7. T. M. Monro, Y. D. West, D. W. Hewak, N. G. R. Broderick, and D. J. Richardson, Electron. Lett. **36**, 1998 (2000).
8. B. T. Kuhlmey, T. P. White, G. Renversez, D. Maystre, L. C. Botten, C. Martijn de Sterke, and R. C. McPhedran, J. Opt. Soc. Am. B **10**, 2331 (2002).
9. B. T. Kuhlmey, "Theoretical and numerical investigation of the physics of microstructured optical fibres," Ph.D. dissertation (Université Aix-Marseille III and University of Sydney, 2003), http://www.physics.usyd.edu.au/~borisk/physics/thesis.pdf.
10. B. T. Kuhlmey, R. C. McPhedran, C. M. de Sterke, P. A. Robinson, G. Renversez, and D. Maystre, Opt. Express **10**, 1285 (2002).
11. A free implementation of the multipole method is available at http://www.physics.usyd.edu.au/cudos/mofsoftware/.
12. T. A. Birks, D. M. Bird, T. D. Hedley, J. M. Pottage, and P. St. J. Russell, Opt. Express **12**, 69 (2003).